

Susceptibility-weighted Imaging Using Susceptibility Map Estimated by L1 Norm Regularization

Ryota Sato¹, Toru Shirai¹, Yo Taniguchi¹, Yoshihisa Soutome¹, and Yoshitaka Bito¹
¹Central Research Laboratory, Hitachi, Ltd., Kokubunji, Tokyo, Japan

Introduction

Susceptibility-weighted imaging (SWI) [1] is widely used to enhance contrast of regions with high magnetic susceptibility, such as veins and iron depositions. However, the contrast produced by SWI changes according to slice orientation, because SWI uses phase, which depends on slice orientation, to enhance contrast. Recently, a new method named "tSWI" was proposed [2]. Although tSWI resolves the dependency of SWI contrast on slice orientation by using an estimated susceptibility map, we previously found that tSWI shows non-local streaking artifacts, especially in slices parallel to the magnetic field, owing to the regularized inverse-filtering procedure used for estimating susceptibility [3]. With tSWI, it is therefore difficult to enhance contrast without causing artifacts in slices parallel to the magnetic field. In this study, to realize susceptibility-weighted imaging in arbitrary slice orientation, a method for susceptibility-weighted imaging, using a susceptibility map estimated by L1 norm regularization, is proposed. Because the proposed method produces no streaking artifacts and attains high contrast-to-noise ratio in arbitrary slice orientation, it can enhance contrast of regions with high magnetic susceptibility in arbitrary slice orientation.

Method

Proposed method Firstly, a susceptibility map is estimated from high-pass filtered phase image by L1 norm regularization based on equation (1) [4],

$$\chi = \operatorname{argmin}_{\chi} \|W(\phi - C\chi)\|_2^2 + \lambda \|\chi\|_1, \quad (1)$$

where W denotes a weight derived from the absolute image, ϕ denotes phase image, χ denotes a susceptibility map, C denotes a matrix representing a convolution with unit dipole magnetic field, and λ denotes constant. The second term in Equation (1) affects susceptibility values nonlinearly and suppresses background noise and streaking artifacts while maintaining high susceptibility values (such as those of veins). χ was calculated from Equation (1) iteratively using a non-linear conjugate gradient method. Secondly, a susceptibility mask $M(i)$ was calculated from susceptibility $\chi(i)$ by using a threshold χ_M as follows: $M(i) = (-\chi_M/\chi(i) + 1)^n$ if $0 < \chi(i) < \chi_M$ where n denotes the number of multiplications. If $\chi < 0$, $M(i)$ is set to 1, and if $\chi > 0$, $M(i)$ is set to 0. χ_M is set to a value that corresponds to the threshold of a phase mask used in SWI. The standard deviations of the susceptibility distribution (σ_χ) and the phase distribution (σ_ϕ) were used to set χ_M to $\pi \cdot \sigma_\chi / \sigma_\phi$. Lastly, susceptibility mask M was multiplied to the absolute image. **Numerical simulations** SWI and the proposed method were applied to simulated phase images of a vein model (which was used because vein contrast is the most dependent on slice orientation in the case of all tissues). The phase images of the model were simulated by the method outlined in [5]. To investigate contrast obtained by SWI and the proposed method in the case of arbitrary slice orientation, slice orientation was changed from coronal to axial (namely, changing angle θ between slice orientation and magnetic field direction by zero, 22.5, 45, 67.5, and 90 degrees) by using the central axis of the vein as a rotation axis. The parameters of the model are as follows: susceptibility difference between a vein and another: 0.2 ppm; diameter of vein: 1 mm; and voxel size: 0.5 × 0.5 × 0.5 mm. **Experiments** SWI, tSWI, and the proposed methods were applied to measurements of healthy volunteers. All experiments were performed on a 1.5T MRI (Echelon Vega, Hitachi Medical Corporation, Japan) equipped with an eight-channel phased-array coil positioned around the head. The scan parameters in axial and coronal slices are as follows: Sequence: RSSG-EPI (RF spoiled-steady state acquisition with rewind gradient echo - echo planar imaging), TR/effective TE = 65/40 ms; NSA = 2; FA = 25; matrix: 512 × 384 × 40; reconstruction matrix: 512 × 512 × 80; and FOV: 220 × 220 × 80 mm. **Processing** After removal of the low-spatial-frequency components of the background phase by performing high-pass filtering for each slice, noise in the air region in the phase image was removed by thresholding. This preprocessed phase image was processed by SWI [1], tSWI [2], and the proposed method. In the case of tSWI, a k-space truncation value, χ_M , and n were set to 0.1, 0.8 ppm, and 4, respectively. As for the proposed method, λ , n , and number of iterations were set to 10^{-3} , 3, and 10, respectively. In the case of all methods, minimum intensity projection (minIP) was carried out over 15 mm around red nuclei. **Evaluation** Numerical simulation was used to examine image contrasts in arbitrary slice orientation acquired by the proposed method in comparison with that acquired by SWI. Head-image experiments with healthy volunteers were used to compare image contrasts of axial and coronal slices acquired by SWI [1], tSWI [2], and the proposed method.

Results and Discussion

As shown in Figures 2(a)-(j), the proposed method clearly enhances the contrast of the vein in each slice orientation, while SWI cannot do so for angle θ of less than 45 degrees. In other words, the proposed method can enhance contrast in arbitrary slice orientation. As shown in Figures 3(a)-(c), in the case of an axial slice, the proposed method can visualize veins and iron depositions as well as SWI and tSWI can, and it shows less background inhomogeneity than SWI and tSWI (blue arrows). In a coronal slice, as shown in Figure 4(a), SWI enhances the surrounding of iron depositions in red nuclei (white arrows) and does not visualize veins clearly (blue arrows). As shown in Figure 4(b), streaking artifacts (red arrows) and shading (green arrows) are observed in the case of tSWI. As shown in Figure 4(c), the proposed method enhances contrast of veins (blue arrows) and iron depositions (white arrows) without causing artifacts.

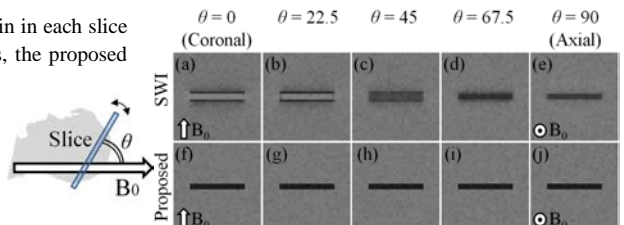


Fig. 1 (left): Schematic view of angle θ between slice orientation and magnetic field direction B_0 . Fig. 2 (right): Simulated results of vein images in arbitrary slice orientation: (a)-(e) SWI, (f)-(j) proposed method.

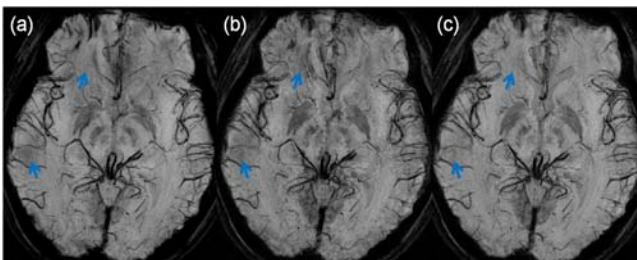


Fig. 3: Axial images of a healthy volunteer by (a) SWI, (b) tSWI, and (c) proposed method.

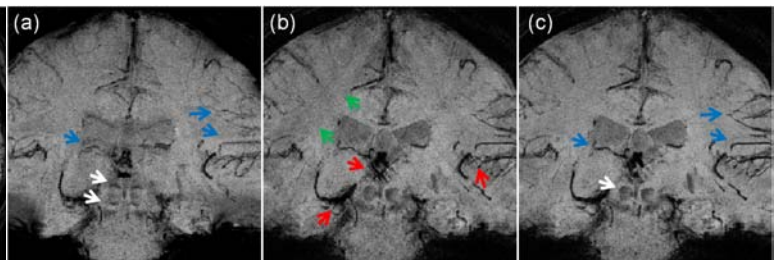


Fig. 4: Coronal images of a healthy volunteer by (a) SWI, (b) tSWI, and (c) proposed method.

Conclusion

Numerical simulation and experiments on healthy volunteers show the proposed method can enhance contrast of regions with high magnetic susceptibility, such as veins or iron depositions, in arbitrary slice orientation.

References

- [1] Haacke, et al. MRM 2004;52:612
- [2] Mork, et al. ISMRM 2012;2366
- [3] Tang, et al. MRM 2012 *in press*.
- [4] Kressler, et al. IEEE TMI 2010;29(2):273
- [5] Marques and Bowtell, Concepts Magn. Reson. Part B 2005;25(1):65